Optimum Combination of Spectral Variables for Crop Mapping in Heterogeneous Landscapes based on Sentinel-2 Time Series and Machine Learning

José Galdino de Oliveira Júnior [1]; Júlio César Dalla Mora Esquerdo [1,2] & Rubens Augusto Camargo Lamparelli [1,3]

[1] UNICAMP - Universidade Estadual de Campinas, Brazil;
[2] Embrapa Agricultura Digital, Brazil;
[3] NIPE - Núcleo Interdisciplinar de Planejamento Energético, Brazil

Keywords: Remote sensing, Random Forest, SITS, Red Edge, agricultural monitoring.

Abstract

This article aimed to determine a workflow for more efficient large-scale crop mapping using a time series of images from the Sentinel-2 Satellite, statistical methods of attribute selection, and machine learning. The proposed methodology explores the best possible combination of spectral variables related to vegetation (16 vegetation indices in the RGB, NIR, SWIR, and Red Edge regions) to characterize different spectro-temporal profiles of Land Use and Land Cover (LULC) in spatially heterogeneous landscapes. First, we applied a data dimensionality reduction analysis using the PCA (Principal Component Analysis) method. Subsequently, the variables that showed the highest statistical correlation between each other were used in the spectro-temporal classification process, using the Random Forest, TempCNN, and LightTAE algorithms, following three different strategies: C1 (ALL), C2 (BE + IV $_{(\text{Red Edge})}$) and C3 (BE + IV $_{(\text{without Red Edge})}$), where ALL – All variables; BE – Spectral Bands; IV – Vegetation Indices. Given the results found, the C2 classification scenario (with bands B3, B4, B5, B6, B7, B8, and B8A and the NDRE1, RESI, and MSR indexes) demonstrated the best LULC classification accuracy at the crop pattern level, compared to the other scenarios, with average values of 0.91, 0.88, 0.91, 0.89, and 0.89 (Global Accuracy, Producer Accuracy, User Accuracy, Kappa index, and F1-Score, respectively, for the TempCNN model), the which emphasized the importance of both qualitative and quantitative variability of sampling data and variables based on the Red Edge region for improving LULC classification processes in large-scale heterogeneous landscapes.

1. Introduction

Agricultural monitoring is a fundamental step for effective decision-making in the field, both concerning production management and the reduction of harmful impacts on the environment arising from the intensification of agricultural practices (Ajadi et al., 2021; Wang et al., 2021; Pott et al., 2022). However, the efficiency of crop monitoring, especially on a large scale, depends on the correct use of strategies for extracting, manipulating, and processing sample data.

Among the most common monitoring methods is information extraction regarding production cycles, carried out directly in the field through occasional and recurring technical visits (Talukdar et al., 2020). However, obtaining this sample data is still subject to limiting factors such as high operational costs and high time consumption to carry out this process (Pott et al., 2021; Mahlayeye; Darvishzadeh and Nelson, 2022). On the other hand, remote sensing data (orbital, suborbital, or proximal) makes it possible to obtain multiple relevant information from the Earth's surface mapping with a more suitable temporal frequency.

Specifically, in studies on the estimation of agricultural production, remote sensing can obtain several aspects intrinsic to the biophysical characteristics of vegetation present in the field, such as level of plant phenology, occurrence of water stress, impact of seasonal climate changes on cycles production, crop productivity prediction, among others (Mercier et al., 2020; Debella-Gilo; Gjertsen, 2021). It can result in a considerable reduction in operational costs related to carrying out large-scale agricultural monitoring (Wang et al., 2023).

Arslan, Topakci & Demir (2022), on the other hand, reinforce that mapping and monitoring such spatio-temporal changes become a difficult task in tropical countries with large territorial extensions, such as Brazil, especially due to the greater presence of clouds in these regions. (Prudente et al., 2020). Furthermore, the main Brazilian LULC monitoring systems that currently exist, such as the TerraClass (Almeida et al., 2016) and MapBiomas (Souza et al., 2020) projects, are mainly based on orbital sensors of low to medium spatial resolution, which makes it possible to extract a variety of accurate information about the Earth's surface. However, there is still a difficulty related to detecting production at the level of agricultural culture and on a large scale, especially in areas that present different cultivation patterns in the same harvest, mainly due to the similarity of the spectro-temporal profiles of some crops (Chen et al., 2018; Picoli et al., 2018).

Nevertheless, the most recent orbital satellite constellations, such as those belonging to the Sentinel series, by presenting different types of sensors with high spatial and temporal resolution, bring new possibilities for long-term environmental monitoring activities, such as the classification of LULC through satellite image time series data (Drusch et al., 2012; Zhao et al., 2022). Moreover, the Sentinel-2 Satellite presents three bands in the Red Edge spectral region, which can help in obtaining more pertinent information for differentiating agricultural vegetative canopies present in a given area, for example (Wei et al., 2023).

Garnot, Landrieu & Chehata (2022) executed an extensive review of the possible ways of combined use of time series of orbital data and described different strategies for certain types of tasks related to LULC classification. These strategies are mainly based on the specific use of machine and deep learning

This contribution has been peer-reviewed. The double-blind peer-review was conducted on the basis of the full paper.
https://doi.org/10.5194/isprs-annals-X-3-2024-85-2024 | © Author(s) 2024. CC BY 4.0 License.

techniques (Yuan and Lin, 2020). Among machine learning algorithms, Random Forest stands out among the others because it generally presents greater versatility in different LULC classification processes, even though it is unable to assimilate information in the temporal dependence of multitemporal sample data (Talukdar et al., 2020; Machichi et al., 2023). Furthermore, because many of these multitemporal data classification methods are still at the state of the art, it is necessary to evaluate their capabilities in more specific tasks such as the spectro-temporal characterization of heterogeneous landscapes, i.e., areas with high spatial and temporal variability in land use and cover.

Therefore, this paper aims to characterize the best combination of spectral variables for large-scale mapping of LULC in heterogeneous landscapes at the level of agricultural cultivation patterns through a temporal series of images from the Sentinel-2 satellite.

2. Materials and Method

The area evaluated in this study is approximately 11,150 km^2. It encompasses, almost in its entirety, the municipality of Rio Verde, Goiás, which was the largest soybean producer in the Southwest Goiás microregion, with a planted area of approximately 410,000 ha and a total production of 1,476,000 tons of this grain in the 2020/2021 harvest (BIGS, 2023). This study area is represented between coordinates 17°12’ to 18° S and 50°30’ to 51°30’ W in Figure 1.

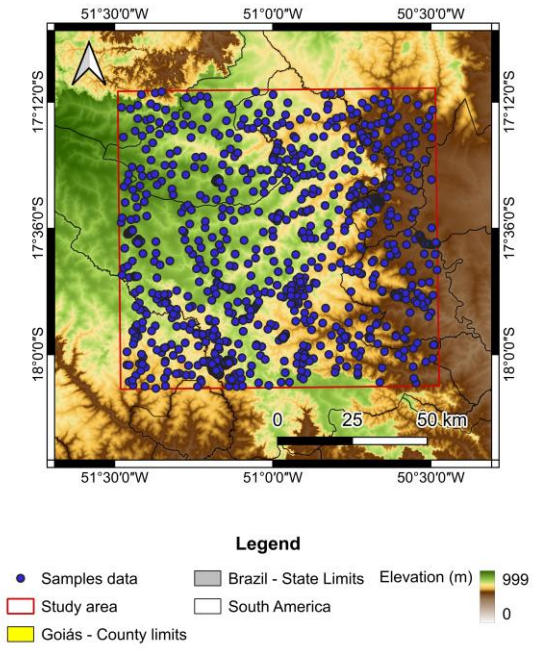

Figure 1. Spatial location of the study area.

The climate of this region is tropical with dry winter (Aw), according to the Köppen-Gieger classification, with an average annual temperature variation of 22 to 24°C and precipitation varying between 1600 and 1900 mm/year (Alvares et al., 2013). The soils in this region are mostly classified as Red Oxisols (Acriferric, Ferric, and Dystrophic), with flat and gently undulating relief (Santos et al., 2018; BIGS, 2019). The main crops produced in this region are sugar cane (*Saccharum officinarum*), soybeans (*Glycine max L.*), and corn (*Zea mays*), with their agricultural calendars extending from September to July, depending on the type of soil, the topography of the land, cultivation pattern and the variation of the dry and rainy climatic seasons (Santos et al., 2021a).

Given this, the methodology of this study consisted of the following steps: Collection of reference sample data and orbital data from the digital platforms of the TerraClass (Almeida et al., 2016), MapBiomas (Souza et al., 2020) projects, SATVeg (Esquerdo et al., 2020) and Brazil Data Cube - BDC (Ferreira et al., 2020); spectral variables calculation (vegetation indexes linked to the RBG, NIR, SWIR and Red Edge regions); analysis of dimensionality reduction of variables and LULC Classification at crop pattern level in R software (R Development Team, 2024).

Firstly, we created a sample database referring to the characteristics of the main LULC classes present in the study area using the TerraClass product (the year 2020), information taken from the SATVeg platform, and the agricultural calendar made publicly available by CONAB (CONAB, 2021). Once we identified such classes, because the TerraClass product only presents biannual data, we need to use the MapBiomas product (the year 2021) to obtain the classes and production cycles that remained for the 2021/2022 harvest (i.e., the type of crops planted, agricultural management system, start and end dates of production harvests). Such specific information is summarized in Table 1 and served as a reference for Sentinel-2 satellite image time series elaboration and the classification process.

ID	Class	Quantity of samples	Percentage of the total database (%)
DC	Double Cropping	277	28.58
OC	One Cropping	112	11.56
PNV	Primary Natural Vegetation	126	13.0
Pt	Pasture	114	11.76
Sc	Silviculture	85	8.77
SNV	Secundary Natural Vegetation	72	7.43
Su	Sugarcane	67	6.91
Ur	Urban area	60	6.19
WB	Water body	56	5.78

Table 1. Tipos de LULC considerados neste estudo.

Next, we created a time series of Sentinel-2 images, spanning the months of September 2021 to August 2022, which were extracted from the orbital database of the BDC project's digital platform (Ferreira et al., 2020). This platform publicly makes time series from several satellites (TERRA and AQUA/MODIS, Landsat 8/OLI, CBERS/AWFI, and Sentinel-2/MSI, among others) available in the ARD – Analysis Ready Data format, which provides the most agile execution of tasks linked to remote sensing and geoprocessing, such as LULC classification. Therefore, there is no need to carry out previous digital pre-processing steps of these orbital data, such as radiometric and atmospheric correction processes (Adrian, Sagan and Maimaitijiang, 2021).

We obtained Sentinel-2 images in 10 spectral bands related to the bands of RGB (490 to 665 nm), Red Edge 1 to 3 (705 to 783 nm), NIR (842 nm), Red Edge 4 (865 nm), SWIR 1 (1,610 nm) and SWIR 2 (2,190 nm), in addition to two other vegetation

indices: the EVI (Enhanced Vegetation Index) and the NDVI (Normalized Difference Vegetation Index).

In addition, 14 vegetation indices (CIre, GNDVI, LSWI, MSR, MTCI, NDRE1, NDRE2, NDRE3, NDSVI, NDTI, RESI, S2REP, SAVI and VARI) were calculated and used in this study, as they were developed to capture the different relationships that exist between vegetation and other types of targets on the Earth's surface; due to non-linear relationships between certain bands of the electromagnetic spectrum of solar radiation. For this reason, they serve as important auxiliary data in the classification of satellite image time series, for example (Jensen, 2011; Pelletier; Webb and Petitjean, 2019).

We chose NDVI, EVI, and SAVI because they are commonly used as essential indices in studies related to the classification of LULC (Rouse et al., 1974; Huete, 1988; Huete et al., 1997; Jensen, 2011; Ienco et al., 2019; Pelletier, Webb and Petitjean, 2019). The LSWI, NDTI and NDSVI are capable of detecting changes in vegetation and soil moisture, being good indicators of changes in the water content of the leaf canopy, such as the presence of water stress or variation in the phenological development of plants (Qi et al., 2002; Xiao et al., 2004; Zhong, Gong and Biging, 2014). The GNDVI, VARI and indices from Red Edge (MSR, MTCI, NDRE, CIre and RESI) were used to detect the different types of vegetative canopies present in the study area through variations in chlorophyll percentages, relating them also at the level of development of plants in the field (Chen, 1996; Gitelson and Merzlyak, 1998; Gitelson et al., 2002; Gitelson et al., 2003; Dash and Curran, 2004; Clevers and Gitelson, 2013; Xiao et al., 2020; Matvienko et al., 2022). S2REP is an adaptation of the REP (Red Edge Position Determination) index for Sentinel-2. It is also an indicator of the chlorophyll content present in the leaf and the stress on the vegetation, depending on the maximum slope between the red and near-infrared spectral bands (Jensen, 2011; Pasternak and Pawluszek-Filipiak, 2022).

The next step consisted of reducing the possibility of insignificance or redundancy of information coming from both the spectral bands of the Sentinel-2 satellite and the vegetation indices used in this article (mainly because some of these indices present, for the most part, information from spectral bands of the red and near-infrared regions). Therefore, it was necessary to apply a statistical analysis to the spectro-temporal sample database created from the time series of orbital data to assess the degree of importance of the variables, aiming to optimize the results obtained by the classifier algorithm (Paul and Kumar, 2019; Pasternak and Pawluszek-Filipiak, 2022; Zhang et al., 2022).

For this task, we used the Principal Component Analysis (PCA) technique, one of the most used methods for statistical analysis related to dimensionality reduction of multivariate data due to its simplicity and operation efficiency. (Gilbertson and Van Niekerk, 2017; Paul and Kumar, 2019; Pasternak and Pawluszek-Filipiak, 2022; Zhang et al., 2022). The PCA technique reduces the number of variables in a database by performing multiple linear combinations. The objective is to keep only the most important variables (i.e., with a high rate of variability between them) in the database and thus avoid redundancy of sample information (Ringnér, 2008; Pasternak and Pawluszek-Filipiak, 2022). These combinations are called Principal Components and can normally describe the behavior of the database variance, about 95%, based on the variables retained in the first three Principal Components (Zhang et al., 2022). This analysis was carried out using the “factoMineR” and “factoextra” packages, both present in the R software. “factoMineR” was used to compute the calculations referring to the PCA analysis, and “factoextra” was used to visualize the results (Lê et al., 2008; Kassambara and Mundt, 2020).

Subsequently, we applied the SOM method (Self-Organizing Maps) to the sample database (Santos et al., 2021b). This procedure was used to avoid the occurrence of errors related to the presence of noisy or incorrectly classified sample points. This technique consists of an unsupervised neural network algorithm that reduces the dimensionality of large databases (such as time series of satellite images), through the topological preservation of the sample data. In this process, this method evaluates the variability of information occurring between samples – both from the same class and from different classes – through a Bayesian inference process (Santos et al., 2021b).

Finally, we performed the classification in three different scenarios: C1 (Spectral bands + all vegetation indices), C2 (Spectral bands + indices based on the Red Edge region only), and C3 (Spectral bands + indices calculated without the Red Edge region), where all scenarios present the variables with quality of representation (cos2) of linear correlation > 0.85, extracted from PCA analysis. The entire classification process was carried out in the R software, using the “SITS” package (Simoes et al., 2021).

The “SITS” package provides the user with a computational interface for manipulating, visualizing, processing, and classifying satellite image time series data (Simoes et al., 2021). This tool features both machine learning and deep learning algorithms, which makes it possible to evaluate different classification strategies. Among all the algorithms in this package, we chose the Random Forest (RF), TempCNN (TC), and LightTAE (LT) algorithms. Random Forest consists of a classifier that employs several decision trees aggregated in joint initialization or bootstrap to reduce the variance of these trees and obtain the final result through an unweighted average majority vote of all trees created. (Breiman, 2001). TempCNN uses a three-layer architecture of sequential 1D convolutional networks in the temporal domain, followed by batch normalizations, a ReLU (Rectified Linear Unit) activation function, and Dropout (Pelletier, Webb and Petitjean, 2019). LightTAE is a temporal attention-based encoding algorithm that is part of a larger architecture that involves the union of a pixel-based spatial encoder with a temporal attention encoder and was developed by Garnot et al. (2020). In this study, 100 trees were used to implement the Random Forest algorithm (Talukdar et al., 2020), while for the TempCNN and LightTAE algorithms, we used the optimization parameters proposed by Camara et al. (2023).

To analyze the performance of the proposed classification scenarios, regarding the spectro-temporal classification accuracy of the study area, we divided the sample data set into two parts (70% - training samples and 30% - test samples), and statistical parameters from the calculation of confusion matrices were used, namely: Global Accuracy (OA), Producer Accuracy (PA), User Accuracy (UA), Kappa index (K) and F1-Score (Yuan and Lin, 2020; Pasternak and Pawluszek -Filipiak, 2022). Equations 1, 2, 3, 4 and 5 describe the calculation for each parameter mentioned above, respectively:

$$OA = \frac{TP + TN}{(TP + TN + FP + FN)} \quad (1)$$

$$PA = \frac{TP}{TP + FN} \quad (2)$$

$$UA = \frac{TP}{TP + FP} \quad (3)$$

$$K = \frac{P_o - P_e}{1 - P_e} \quad (4)$$

$$F1_{Score} = \frac{2 \times PA \times UA}{PA + UA} \quad (5)$$

Where:

TP – Number of sample points of the true class correctly classified;
TN – Number of sample points truly classified in another class;
FN – Number of sample points from the true class that the algorithm misclassified into another class;
FP – Number of sample points that the algorithm incorrectly classified into the true class;
P_o – Probability observed by classification;
P_e – Expected probability for classification.

The OA consists of the set of sample points correctly classified as the total number of sample points. The PA and UA represent the correctly classified sampling points considering the errors of omission and commission for each land use and cover class. The Kappa index was developed by Cohen (1960) and is used in remote sensing as a metric for evaluating the general accuracy of a classification. F1-Score is a harmonic average between the PA and UA, aiming to obtain a single evaluation parameter with better statistical performance compared to the previous ones (Yuan and Lin, 2020; Nasiri et al., 2022).

3. Results and Discussion

After performing the dimensionality reduction analysis of the spectral variables, we observed that approximately 86.7% of the variance in the sample data was found in the first three main components or PCA dimensions (Figure 2A).

Regarding the percentage of contribution of the variables, the spectral bands B03, B04, B05, B06, B07, B08, and B8A and the vegetation indices SAVI, NDRE1, MSR, RESI, and NDVI presented the highest values among the others, being approximately variable between 4.4% and 5% (Figure 2B).

It indicated that, in general, the indices based on simple algebraic normalization relationships between the red (B04) and near-infrared (B05, B06, B07, and B08) regions were sufficient to explain much of the correlation between these indices and variability of the spectral behavior of the sample data. Furthermore, the presence of three indices based on the Red Edge region (NDRE1, MSR, and RESI) initially revealed the greater influence of this spectral region on this correlation between the sample data. Zhang et al. (2020), Zhang et al. (2021), and Chaves & Sanches (2023) found similar results in their respective studies, which also emphasized the relevance of Red Edge bands in the classification process at the crop level.

On the other hand, the first two dimensions expressed around 77% of the variability in the behavior of the sample data (Figure 3), indicating that these variables above were also the most important among the others evaluated.

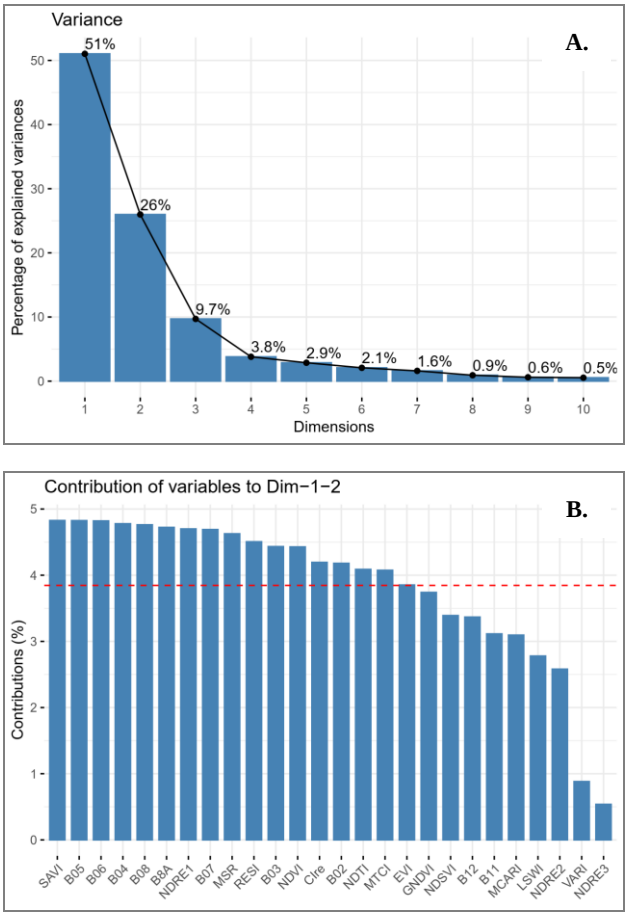

Figure 2. Percentages of variance (A) and contribution of variables (B) regarding the behavior of the sample data, depending on the dimensions originated by the PCA method.

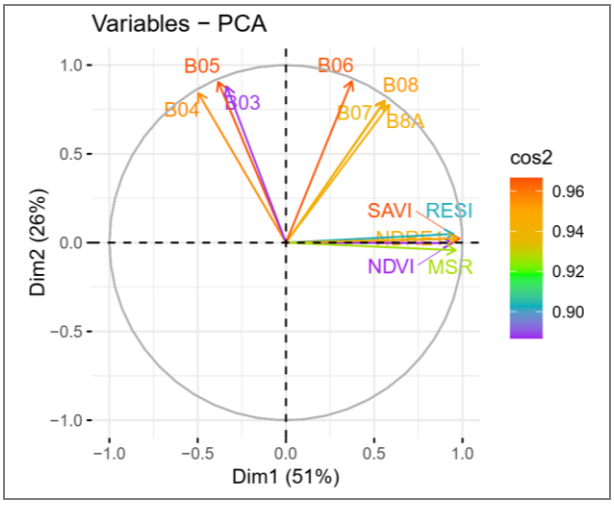

Figure 3. Ordering diagram of variables at the cos2 > 0.85, correlating the first two PCA dimensions.

These variables presented a quality of representation (cos2) greater than 0.85 in the ordination diagram composed of the first two PCA dimensions and, therefore, presented the highest linear correlation values between the other variables analyzed. Therefore, these variables were chosen for the LULC classification process in the three scenarios already mentioned (C1, C2, and C3).

This contribution has been peer-reviewed. The double-blind peer-review was conducted on the basis of the full paper.
https://doi.org/10.5194/isprs-annals-X-3-2024-85-2024 | © Author(s) 2024. CC BY 4.0 License.

When applying the SOM method to the sample database composed of the variables with the highest linear correlation between each other (according to PCA analysis), we noticed that there was a reduction of approximately 17.2%, 19% and 17.8% for scenarios C1, C2 and C3, respectively (Table 2).

		Number of samples per scenario			
ID	**Class**	**Original Base**	**C1**	**C2**	**C3**
DC	Double Cropping	277	250	242	250
OC	One Cropping	112	69	59	69
PNV	Primary Natural Vegetation	126	118	117	112
Pt	Pasture	114	91	97	96
Sc	Silviculture	85	55	56	58
SNV	Secundary Natural vegetation	72	65	60	57
Su	Sugarcane	67	45	42	46
Ur	Urban area	60	53	57	53
WB	Water body	56	56	56	56
TOTAL		969	802	786	797
Sample reduction percentage (%)		-	17,2	19	17,8

Table 2. Comparison of the sampling base before and after applying the SOM method for each classification scenario.

This fact demonstrated that scenario C2 suffered the greatest reduction in samples compared to the other scenarios, which would initially lead to the assumption that there was a decrease in accuracy in the classification process. However, how this scenario only uses indices based on the Red Edge region and that most of the chosen spectral bands also belong to this spectral region, what caused better differentiation of the spectro-temporal profiles of the different types of uses and existing land cover in the study area (Mahlayeye et al., 2022).

This assumption was proven when we evaluated the statistical metrics originating from the classification process. We achieved the best results precisely when we prioritized vegetation indices based on the Red Edge region in the learning process of the classifier algorithms. Furthermore, the TempCNN algorithm presented the best overall result with OA, K, and F values equal to 0.91, 0.89, and 0.89, respectively (Table 3).

			Machine Learning Models		
			RF	TC	LT
Classification Scenarios	C1	OA	**0.89**	0.83	0.71
		K	**0.86**	0.80	0.66
		F	**0.86**	0.79	0.70
	C2	OA	**0.90**	**0.91**	**0.86**
		K	**0.88**	**0.89**	**0.84**
		F	**0.88**	**0.89**	**0.86**
	C3	OA	**0.85**	0.82	0.82
		K	**0.82**	0.79	0.79
		F	**0.82**	0.80	0.81

Table 3. Acurácia global (OA), Kappa Index (K) e F1-score (F) médios para todos os cenários e algoritmos de classificação.

However, except for this best result achieved by the TC model, the RF model achieved the best accuracy for all classification scenarios (Table 3). Furthermore, the RF model finished the classification process for the C2 scenario in minor time (1 hour and 5 minutes), compared to the TC model (20 hours and 35 minutes). These observations highlight the greater efficiency of the Random Forest algorithm, compared to the TempCNN and LightTAE models, in extracting relevant information from scarce sample databases with high similarity of spectro-temporal patterns of different types of land use and cover, as also described by Moskolai et al. (2021) in their study, where they cited the need for bigger database for deep learning algorithms to function correctly.

This consideration could be proven when we evaluated the producer and user accuracies, class by class, for these two algorithms in question, RF and TC models (Figure 4). Where we realize that the RF model, even though the producer's accuracy is slightly lower than the TC model (specifically, due to the values achieved for the Pasture, Sugarcane, and Silviculture classes), the latter still achieved better efficiency in the differentiation of the multiple types of vegetative canopies present in the study area, since, the Random Forest algorithm obtained higher user accuracy values for the One Cropping, Silviculture, and Sugarcane classes (Figure 4B).

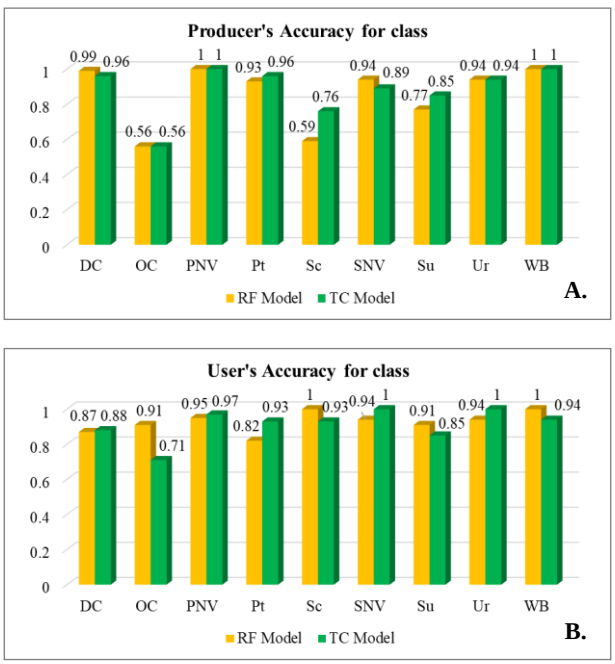

Figure 4. Comparison of Producer Accuracy (PA) and User Accuracy (UA) for the RF and TC models, considering the C2 classification scenario and all LULC classes used in the study.

However, these observations only reinforced that both classifier algorithms achieved excellent results from the multi-temporal spectral band data and vegetation indices combination based on the Red Edge spectral region.

4. Conclusions

The variables (B03, B04, B05, B06, B07, B08, B8A, NDRE1, RESI, and MSR) related to the TempCNN algorithm performed the most suitable strategy for classifying changes in land use and cover at the level of cultivation pattern and on a large scale, considering the conditions of this experiment. However, we also

This contribution has been peer-reviewed. The double-blind peer-review was conducted on the basis of the full paper.
https://doi.org/10.5194/isprs-annals-X-3-2024-85-2024 | © Author(s) 2024. CC BY 4.0 License.

advise Random Forest as an alternative option, due to its excellent performance given the limiting settings of this study: a scarce database with high interclass similarity of spectro-temporal patterns. Therefore, we emphasize that such considerations are mainly due to the efficient previous steps of sampling manipulation, making such findings very relevant and can directly impact the processing time and operational costs in tasks linked to agricultural monitoring using remote sensing today.

Acknowledgements

The authors would like to thank the institutions UNICAMP – Universidade Estadual de Campinas and CAPES – Coordenação de Aperfeiçoamento de Pessoal de Nível Superior for the technical-financial resources that made this work possible.

References

Adrian, J., Sagan, V., Maimaitijiang, M., 2021. Sentinel SAR-optical fusion for crop type mapping using deep learning and Google Earth Engine. *ISPRS Journal of Photogrammetry and Remote Sensing*, 175, 215-235. https://doi.org/10.1016/j.isprsjprs.2021.02.018.

Ajadi, O. A. et al., 2021. Large-scale crop type and crop area mapping across Brazil using synthetic aperture radar and optical imagery. *International Journal of Applied Earth Observation and Geoinformation*, 97, 102294. https://doi.org/10.1016/j.jag.2020.102294.

Almeida, C.A. de et al., 2016. High spatial resolution land use and land cover mapping of the Brazilian legal Amazon in 2008 using Landsat-5/TM and MODIS data. *Acta Amazonica*, 46(3), 291-302. https://doi.org/10.1590/1809-4392201505504.

Alvares, C.A. et al., 2013. Köppen’s climate classification map for Brazil. *Meteorologische Zeitschrift*, 22(6), 711-728. https://doi.org/10.1127/0941-2948/2013/0507.

Arslan, İ., Topakci, M., Demir, N., 2022. Monitoring Maize Growth and Calculating Plant Heights with Synthetic Aperture Radar (SAR) and Optical Satellite Images. *Agriculture* (Switzerland), 12(6), 800. https://doi.org/10.3390/agriculture12060800.

BIGS. Brazilian Institute of Geography and Statistics. SIDRA – Sistema IBGE de Recuperação Automática. 2023. Available in: https://sidra.ibge.gov.br/home/ipp/brasil.

BIGS. Brazilian Institute of Geography and Statistics. Maps portal: Pedology. 2019. Available in: https://portaldemapas.ibge.gov.br/portal.php#mapa220925.

Breiman, L. 2001. Random Forests. *Machine Learning*, 45, 5-32. https://doi.org/10.1023/A:1010933404324.

Camara, G. et al., 2023. "sits: Satellite Image Time Series Analysis on Earth Observation Data Cubes". Available in: https://e-sensing.github.io/sitsbook/.

Chaves, M.E.D., Sanches, I.D., 2023. Improving crop mapping in Brazil’s Cerrado from a data cubes-derived Sentinel-2 temporal analysis. *Remote Sensing Applications: Society and Environment*, 32, 101014. https://doi.org/10.1016/j.rsase.2023.101014.

Chen, Y. et al., 2018. Mapping croplands, cropping patterns, and crop types using MODIS time-series data. *International Journal of Applied Earth Observation and Geoinformation*, 69, 133-147. https://doi.org/10.1016/j.jag.2018.03.005.

Clevers, J.G.P.W., Gitelson, A.A., 2013. Remote estimation of crop and grass chlorophyll and nitrogen content using red-edge bands on sentinel-2 and-3. *International Journal of Applied Earth Observation and Geoinformation*, 23(1), 344-351. https://doi.org/10.1016/j.jag.2012.10.008.

Cohen, J., 1960. A Coefficient of Agreement for Nominal Scales. *Educational and Psychological Measurement*, 20(1), 37-46. http://dx.doi.org/10.1177/001316446002000104.

CONAB. Companhia Nacional de Abastecimento. Calendário agrícola da safra 2021/2022. 2021. Available in: https://www.conab.gov.br/institucional/publicacoes/outras-publicacoes/item/download/45710_77f0a5ee35e765e2248999f4c61e70c8.

Dash, J., Curran, P.J., 2004. The MERIS terrestrial chlorophyll index. *International Journal of Remote Sensing*, 25(23), 5403-5413. https://doi.org/10.1080/0143116042000274015.

Daughtry, C.S.T. et al., 2000. Estimating Corn Leaf Chlorophyll Concentration from Leaf and Canopy Reflectance. *Remote Sensing of Environment*, 74(2), 229-239. https://doi.org/10.1016/S0034-4257(00)00113-9.

Debella-Gilo, M., Gjertsen, A.K., 2021. Mapping seasonal agricultural land use types using deep learning on sentinel-2 image time series. *Remote Sensing*, 13(2), 289. https://doi.org/10.3390/rs13020289.

Drusch, M. et al., 2012. Sentinel-2: ESA’s Optical High-Resolution Mission for GMES Operational Services. *Remote Sensing of Environment*, 120, 25-36. https://doi.org/10.1016/j.rse.2011.11.026.

Esquerdo, J.C.D.M. et al., 2020. SATVeg: A web-based tool for visualization of MODIS vegetation indices in South America. *Computers and Electronics in Agriculture*, 175, 105516. https://doi.org/10.1016/j.compag.2020.105516.

Ferreira, K.R. et al., 2020. Earth observation data cubes for Brazil: Requirements, methodology and products. *Remote Sensing*, 12(24), 4033, https://doi.org/10.3390/rs12244033.

Garnot, V.S.F., Landrieu, L., 2020. Lightweight Temporal Self-attention for Classifying Satellite Images Time Series. In: Lemaire, V., Malinowski, S., Bagnall, A., Guyet, T., Tavenard, R., Ifrim, G. (eds) *Advanced Analytics and Learning on Temporal Data*. AALTD 2020. Lecture Notes in Computer Science, v. 12588. Springer, Cham. https://doi.org/10.48550/arXiv.2007.00586.

Garnot, V.S.F., Landrieu, L., Chehata, N., 2022. Multi-modal temporal attention models for crop mapping from satellite time series. *ISPRS Journal of Photogrammetry and Remote Sensing*, 187, 294-305. https://doi.org/10.1016/j.isprsjprs.2022.03.012.

Gilbertson, J.K., Van Niekerk, A., 2017. Value of dimensionality reduction for crop differentiation with multi-temporal imagery and machine learning. *Computers and Electronics in Agriculture*, 142, 50-58, https://doi.org/10.1016/j.compag.2017.08.024.

Gitelson, A.A. et al., 2002. Vegetation and soil lines in visible spectral space: A concept and technique for remote estimation of vegetation fraction. *International Journal of Remote Sensing*, 23(13), 2537-2562. https://doi.org/10.1080/01431160110107806.

Gitelson, A.A. et al., 2003. Remote estimation of leaf area index and green leaf biomass in maize canopies. *Geophysical Research Letters*, 30(5). https://doi.org/10.1029/2002GL016450.

Gitelson, A.A., Merzlyak, M.N., 1998. Remote sensing of chlorophyll concentration in higher plant leaves. *Advances in Space Research*, 22(5), 689-692. https://doi.org/10.1016/S0273-1177(97)01133-2.

Guyot, G.; Baret, F., 1988. Utilisation de La Haute Resolution Spectrale Pour Suivre L’etat des Couverts Vegetaux. In: Spectral Signatures of Objects in Remote Sensing, Proceedings of the conference held 18-22 January, 1988 in Aussois (Modane), France. Edited by T.D. Guyenne and J.J. Hunt. ESA SP-287. European Space Agency, 279.

Hu, Q. et al., 2019. A phenology-based spectral and temporal feature selection method for crop mapping from satellite time series. *International Journal of Applied Earth Observation and Geoinformation*, 80, 218-229. https://doi.org/10.1016/j.jag.2019.04.014.

Huete, A.R., 1988. A soil-adjusted vegetation index (SAVI). *Remote Sensing of Environment*, 25(3), 295-309. https://doi.org/10.1016/0034-4257(88)90106-X.

Huete, A. R. et al., 1997. A comparison of vegetation indices over a global set of TM images for EOS-MODIS. *Remote Sensing of Environment*, 59(3), 440-451. https://doi.org/10.1016/S0034-4257(96)00112-5.

Ienco, D. et al., 2019. Combining Sentinel-1 and Sentinel-2 Satellite Image Time Series for land cover mapping via a multi-source deep learning architecture. *ISPRS Journal of Photogrammetry and Remote Sensing*, 158, 11-22. https://doi.org/10.1016/j.isprsjprs.2019.09.016.

Jensen, J. R. Sensoriamento remoto da vegetação. In: Jensen, J. R. *Sensoriamento remoto do ambiente: uma perspectiva em recursos terrestres*. 2. ed. São José dos Campos: Parêntese, Cap. 11, p. 357-410, 2011.

Lê, S. et al., 2008. FactoMineR: An R Package for Multivariate Analysis. *JSS Journal of Statistical Software*. [s.l: s.n.]. Available in: http://www.jstatsoft.org/.

Mahlayeye, M., Darvishzadeh, R., Nelson, A., 2022. Cropping Patterns of Annual Crops: A Remote Sensing Review. *Remote Sensing*, 14(10), 2404. https://doi.org/10.3390/rs14102404.

Machichi, M.A. et al., 2023. Crop mapping using supervised machine learning and deep learning: a systematic literature review. *International Journal of Remote Sensing*, 44(8), 2717-2753. https://doi.org/10.1080/01431161.2023.2205984.

Matvienko, I. et al., 2022. Bayesian Aggregation Improves Traditional Single-Image Crop Classification Approaches. *Sensors*, 22(22), 8600. https://doi.org/10.3390/s22228600.

Mercier, A. et al., 2020. Evaluation of Sentinel-1 & 2 time series for predicting wheat and rapeseed phenological stages. *ISPRS Journal of Photogrammetry and Remote Sensing*, 163, 231-256. https://doi.org/10.1016/j.isprsjprs.2020.03.009.

Moskolai, W.R. et al., 2021. Application of Deep Learning Architectures for Satellite Image Time Series Prediction: A Review. *Remote Sensing*, 13(23), 4822. https://doi.org/10.3390/rs13234822.

Nasiri, V. et al., 2022. Land Use and Land Cover Mapping Using Sentinel-2, Landsat-8 Satellite Images, and Google Earth Engine: A Comparison of Two Composition Methods. *Remote Sensing*, 14(9), 1977. https://doi.org/10.3390/rs14091977.

Pasternak, M., Pawluszek-Filipiak, K., 2022. The Evaluation of Spectral Vegetation Indexes and Redundancy Reduction on the Accuracy of Crop Type Detection. *Applied Sciences* (Switzerland), 12(10), 5067. https://doi.org/10.3390/app12105067.

Paul, S., Kumar, D.N., 2019. Evaluation of Feature Selection and Feature Extraction Techniques on Multi-Temporal Landsat-8 Images for Crop Classification. *Remote Sensing in Earth Systems Sciences*, 2(4), 197-207. https://doi.org/10.1007/s41976-019-00024-8.

Pelletier, C., Webb, G. I., Petitjean, F., 2019. Temporal convolutional neural network for the classification of satellite image time series. *Remote Sensing*, 11(5), 523. https://doi.org/10.3390/rs11050523.

Picoli, M.C.A. et al., 2018. Big earth observation time series analysis for monitoring Brazilian agriculture. *ISPRS Journal of Photogrammetry and Remote Sensing*, 145, 328-339. https://doi.org/10.1016/j.isprsjprs.2018.08.007.

Pott, L.P. et al., 2021. Satellite-based data fusion crop type classification and mapping in Rio Grande do Sul, Brazil. *ISPRS Journal of Photogrammetry and Remote Sensing*, 176, 196-210. https://doi.org/10.1016/j.isprsjprs.2021.04.015.

Pott, L.P. et al., 2022. Crop type classification in Southern Brazil: Integrating remote sensing, crop modeling and machine learning. *Computers and Electronics in Agriculture*, 201, 107320. https://doi.org/10.1016/j.compag.2022.107320.

Prudente, V.H.R. et al., 2020. Limitations of cloud cover for optical remote sensing of agricultural areas across South America. *Remote Sensing Applications: Society and Environment*, 20, 100414. https://doi.org/10.1016/j.rsase.2020.100414.

Qi, J. et al., 1994. A Modified Soil Adjusted Vegetation Index. *Remote Sensing of Environment*, 48(2), 119-126. https://doi.org/10.1016/0034-4257(94)90134-1.

Qi, J. et al., 2002. RANGES improves satellite-based information and land cover assessments in southwest United States. *Eos, Trans. Am. Geophys. Union*, 83(51), 601-606. https://doi.org/10.1029/2002EO000411.

R Development Team., 2023. R Statistical Package: The R Project for Statistical Computing. Available in: https://www.r-project.org/.

Ringnér, M., 2008. What is principal component analysis? Nature Biotechnology. [s.l: s.n.]. Available in: http://www.nature.com/naturebiotechnology.

Rouse, J.W. et al., 1974. Monitoring vegetation systems in the great plains with ERTS. Proceedings Third Earth Resources Tecnology Satellite-1 Symposium. Greenbelt: NASA SP-351, 1974. p. 3010-3017.

Santos, H.G. et al., 2018. Sistema Brasileiro de Classificação de Solos. 5. ed., revisada e ampliada. Brasília – DF: Embrapa, 2018. 356p. Available in: https://www.embrapa.br/solos/sibcs.

Santos, L.A. et al., 2021a. Identifying spatiotemporal patterns in land use and cover samples from satellite image time series. *Remote Sensing*, 13(5), 974. https://doi.org/10.3390/rs13050974.

Santos, L.A. et al., 2021b. Quality control and class noise reduction of satellite image time series. *ISPRS Journal of Photogrammetry and Remote Sensing*, 177, 75-88. https://doi.org/10.1016/j.isprsjprs.2021.04.014.

Simoes, R. et al., 2021. Satellite image time series analysis for big earth observation data. *Remote Sensing*, 13(13), 2428. https://doi.org/10.3390/rs13132428.

Souza, C.M. et al., 2020. Reconstructing three decades of land use and land cover changes in brazilian biomes with landsat archive and earth engine. *Remote Sensing*, 12(17), 2735. https://doi.org/10.3390/RS12172735.

Talukdar, S. et al., 2020. Land-use land-cover classification by machine learning classifiers for satellite observations-A review. *Remote Sensing*, 12(7), 1135. https://doi.org/10.3390/rs12071135.

Wang, Y. et al., 2021. A new attention-based CNN approach for crop mapping using time series Sentinel-2 images. *Computers and Electronics in Agriculture*, 184, 106090. https://doi.org/10.1016/j.compag.2021.106090.

Wang, Y. et al., 2023. An unsupervised domain adaptation deep learning method for spatial and temporal transferable crop type mapping using Sentinel-2 imagery. *ISPRS Journal of Photogrammetry and Remote Sensing*, 199, 102-117. https://doi.org/10.1016/j.isprsjprs.2023.04.002.

Wei, M. et al., 2023. Investigating the Potential of Crop Discrimination in Early Growing Stage of Change Analysis in Remote Sensing Crop Profiles. *Remote Sensing*, 15(3), 853. https://doi.org/10.3390/rs15030853.

Xiao, X. et al., 2004. Satellite-based modeling of gross primary production in an evergreen needleleaf forest. *Remote Sensing of Environment*, 89(4), 519-534. https://doi.org/10.1016/j.rse.2003.11.008.

Xiao, C. et al., 2020. Sentinel-2 red-edge spectral indices (RESI) suitability for mapping rubber boom in Luang Namtha Province, northern Lao PDR. *International Journal of Applied Earth Observation and Geoinformation*, 93, 102176. https://doi.org/10.1016/j.jag.2020.102176.

Yin, L. et al., 2020. Optimizing feature selection of individual crop types for improved crop mapping. *Remote Sensing*, 12(1), 162. https://doi.org/10.3390/RS12010162.

Yuan, Y., Lin, L., 2020. Self-Supervised Pretraining of Transformers for Satellite Image Time Series Classification. *IEEE Journal of Selected Topics in Applied Earth Observations and Remote Sensing*, 14, 474-487. https://doi.org/10.1109/JSTARS.2020.3036602.

Zhang et al., 2020. Accessing the temporal and spectral features in crop type mapping using multi-temporal Sentinel-2 imagery: A case study of Yi’an County, Heilongjiang province, China. *Computers and Electronics in Agriculture*, v. 176, 105618. https://doi.org/10.1016/j.compag.2020.105618.

Zhang, H. et al., 2021. Investigating the impact of classification features and classifiers on crop mapping performance in heterogeneous agricultural landscapes. *International Journal of Applied Earth Observations and Geoinformation*, 102, 102388. https://doi.org/10.1016/j.jag.2021.102388.

Zhang, T. et al., 2022. Rice and Greenhouse Identification in Plateau Areas Incorporating Sentinel-1/2 Optical and Radar Remote Sensing Data from Google Earth Engine. *Remote Sensing*, 14(22), 5727. https://doi.org/10.3390/rs14225727.

Zhao, W. et al., 2022. Spatial-aware SAR-optical time-series deep integration for crop phenology tracking. *Remote Sensing of Environment*, 276, 113046. https://doi.org/10.1016/j.rse.2022.113046.

Zhong, L., Gong, P., Biging, G.S., 2014. Efficient corn and soybean mapping with temporal extendability: A multi-year experiment using Landsat imagery. *Remote Sensing of Environment*, 140, 1-13. https://doi.org/10.1016/j.rse.2013.08.023.

Zhu, A.X. et al., 2021. Mapping rice paddy distribution using remote sensing by coupling deep learning with phenological characteristics. *Remote Sensing*, 13(7), 1360. https://doi.org/10.3390/rs13071360.